

Towards A Consistent Modeling Of Protein Thermodynamic And Kinetic Cooperativity: How Applicable Is The Transition State Picture To Folding and Unfolding?

Hüseyin KAYA and Hue Sun CHAN
*Department of Biochemistry, and
 Department of Medical Genetics & Microbiology
 Faculty of Medicine, University of Toronto
 Toronto, Ontario M5S 1A8, Canada*

To what extent do general features of folding/unfolding kinetics of small globular proteins follow from their thermodynamic properties? To address this question, we investigate a new simplified protein chain model that embodies a cooperative interplay between local conformational preferences and hydrophobic burial. The present four-helix-bundle 55mer model exhibits proteinlike calorimetric two-state cooperativity. It rationalizes native-state hydrogen exchange observations. Our analysis indicates that a coherent, self-consistent physical account of both the thermodynamic and kinetic properties of the model leads naturally to the concept of a native state ensemble that encompasses considerable conformational fluctuations. Such a multiple-conformation native state is seen to involve conformational states similar to those revealed by native-state hydrogen exchange. Many of these conformational states are predicted to lie below native baselines commonly used in interpreting calorimetric data. Folding and unfolding kinetics are studied under a range of intrachain interaction strengths as in experimental chevron plots. Kinetically determined transition midpoints match well with their thermodynamic counterparts. Kinetic relaxations are found to be essentially single exponential over an extended range of model interaction strengths. This includes the entire unfolding regime and a significant part of a folding regime with a chevron rollover, as has been observed for real proteins that fold with non-two-state kinetics. The transition state picture of protein folding and unfolding is evaluated by comparing thermodynamic free energy profiles with actual kinetic rates. These analyses suggest that some chevron rollovers may arise from an internal frictional effect that increasingly impedes chain motions with more native conditions, rather than being caused by discrete deadtime folding intermediates or shifts of the transition state peak as previously posited.

Running title: Transition State Picture of Protein Folding

Key words: calorimetric cooperativity / single-exponential kinetics / rugged landscape / unfolding / chevron plot / four-helix bundle / heat capacity / lattice protein models

I. INTRODUCTION

Our physical knowledge of protein folding is measured by the extent to which current ideas of elemental polypeptide interactions are capable of reproducing experimental data. Tremendous experimental progress has been made in the recent past.^{1–6} During the same time, investigations of simplified self-contained polymer models have contributed much physical insight.^{7–16} These models are successful in physically rationalizing many general features of proteins in terms of polymer properties, building a foundation for future advances. To move forward in theoretical development, it is necessary to recognize what common protein properties have not been predicted by models to date and target our efforts towards rectifying such deficiencies. A prime example is the current lack of chain models that can quantitatively reflect the extreme kinetic and thermodynamic cooperativity of small single-domain proteins.^{5,17} This highlights our insufficient understanding of protein energetics even at a “big-picture” level, suggesting that as heteropolymers natural proteins may be quite special in some respects.

We have recently investigated the severe constraints imposed on protein polymer models by the experimental observations of calorimetric and other hallmarks of thermodynamic two-state cooperativity.^{18–20} These cooperativity requirements appear to be more stringent than most other generic protein properties studied so far. A variety of flexible heteropolymer models with additive residue-based contact energies are able to explain significant aspects of the folding process.^{7–16} But such additive models — at least for the several examples evaluated to date — are found to be insufficient to satisfy the thermodynamic cooperativity requirements, even though deviations from proteinlike thermodynamics can be lessened in some instances by enhancing interaction heterogeneity through using larger numbers of letters and repulsive energies in model alphabets.¹⁹ As far as thermodynamic cooperativity is concerned, in scenarios tested thus far, we find that proteinlike thermodynamics can arise from non-additive cooperative contributions that originate from an interplay between local conformational preferences and (mostly nonlocal) interactions that favor formation of protein cores.^{18,20}

In the folding literature, an intimate correspondence between protein thermodynamics and kinetics has figured prominently in theoretical,^{7,21–23} modeling,^{24–27} and interpretative^{2,4} discourses. Therefore, we ask: Given that a heteropolymer model has already been constrained to satisfy a set of proteinlike thermodynamic properties, to what extent proteinlike kinetic behavior would follow automatically? For instance, would such a model be sufficient for two-state kinetics as observed for many small single-domain proteins⁵? More generally, what improvement in proteinlike kinetics would such a model enjoy over other models that are now known to be thermodynamically less cooperative?

In analyses of folding/unfolding kinetics experiments, free energy profiles are used extensively to provide useful insight^{2,4,28–33} and as a picturesque device to summarize data. However, other than the folding free energy and rate measurements themselves, independent experimental techniques to accurately define and determine such profiles are currently lacking. Moreover, many of these profiles were proposed without considering explicit chain representations. Therefore, the applicability and generality of their implied physical pictures remain to be ascertained. Coarse-grained protein chain models are well suited to shed light on this fundamental issue because they allow for broad conformational sampling. Free energy profiles in coarse-grained models can be obtained directly from chain population distributions, without regard to (and therefore independent of) kinetic rates. It follows that a rigorous evaluation of the applicability of transition state theory to protein folding can be conducted by comparing the transition-state-predicted rates and the actual kinetic rates in these models. We study one such model below.

II. A MODEL FOR THERMODYNAMIC COOPERATIVITY

The present analysis is based on a thermodynamically cooperative 55mer lattice protein model that folds to a ground state with a four-helix core (Fig. 1). The intrachain interaction scheme includes additive 5-letter contact energies,^{20,34} repulsive interactions disfavoring left-handed helices and sharp turns at the end of a helix, as well as cooperative “native hydrogen bond burial” terms²⁰ (c.f. refs. 35, 36). The total energy E is defined by Eq. (1) in ref. 20. Although “native-centric” interactions were introduced to enhance thermodynamic cooperativity in the present model, unlike the usual Gō construction, they are not necessary for recognizing the ground state. This is because the general, non-native-centric terms in the model (all terms in E except the “native hydrogen bond burial” terms) are sufficient to provide global favorability to the proteinlike four-helix ground state. We note that several other studies^{36–39}

have also emphasized cooperative interactions in protein folding; and nonadditive aspects of hydrophobic effects are being explored.^{40–45} As we have emphasized,²⁰ although the present model is useful for exploring the issues at hand, it should be regarded as tentative, partly because it does not provide an explicit account of other possible physical origins of protein thermodynamic cooperativity such as sidechain packing.^{19,46,47} Furthermore, in view of the current lack of definitive understanding of hydrogen bonding energetics (see discussion and references in ref. 20), the cooperative “native hydrogen bond burial” energy in the present model should be broadly interpreted as representative of a general favorable coupling between local conformational preference and formation of proximate tertiary contacts, the physical mechanisms of which remain to be further elucidated.

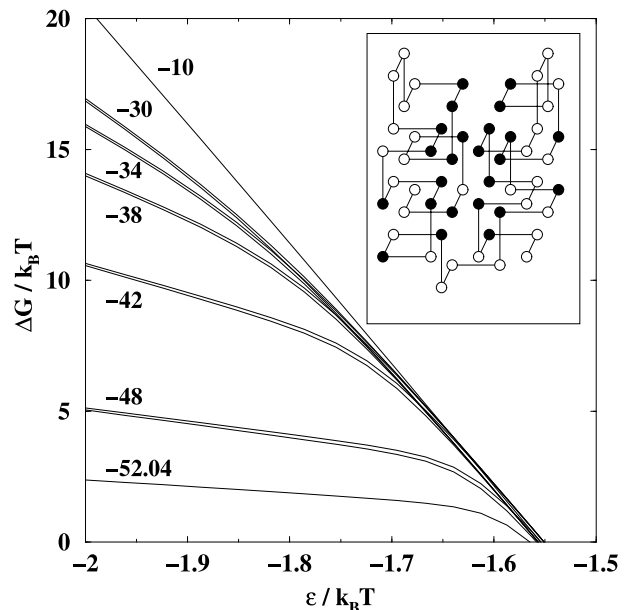


FIG. 1. Thermodynamic stabilities and definitions of native and denatured states. One of the eight iso-energetic ground-state conformations is shown in the inset, where black beads denote nominally hydrophobic residues.²⁰ Free energies of unfolding $\Delta G = k_B T \ln(P_N/P_D)$. Solid curves (labeled by E_t) classify conformations with $E \leq E_t$ and $E > E_t$ as native and denatured, respectively. Dashed curves show the free energy of denatured conformations, defined as those with E greater than the values shown, relative to the ground-state-only native state with $E_t = -52.04$. All results presented in this paper were obtained using model energetic parameters $\gamma_{lh} = 6.0$, $\gamma_{st} = 5.0$, $\mathcal{E}_{\text{Helix}} = 0$, $b\mathcal{E}_{\text{Hb}} = -0.8$, and $b = 1.5$ as specified ref. 20.

In addition to the formulation in ref. 20, here we introduce a parameter ϵ to model protein behaviors at different intrachain interaction strengths, such that the *effective* energy of a conformation with energy E is equal to $-\epsilon E$, hence its Boltzmann weight equals $\exp(\epsilon E/k_B T)$, where $k_B T$ is Boltzmann’s constant times absolute tem-

perature. It follows that the partition function $Q = \sum_E g(E) \exp(\epsilon E/k_B T)$, where $g(E)$ is the number of conformations with energy E , and $g(E)$ is estimated by a parameter-space Monte Carlo histogram technique.²⁰ The formulation in ref. 20 corresponds to $\epsilon = -1$. Because of the peculiar and significant temperature dependence of the solvent-mediated interactions in real proteins, varying $-\epsilon/k_B T$ serves better as a model for how effective intrachain interactions are modulated at constant temperature by denaturant concentration⁴⁸ or denaturant activity³⁷ than for how Boltzmann weights changes with temperature.^{11,49–51} Here, as a first approximation, denaturant effects are simply taken to be uniform over different interaction types. Models with different denaturant effects on different interaction types remain to be explored.

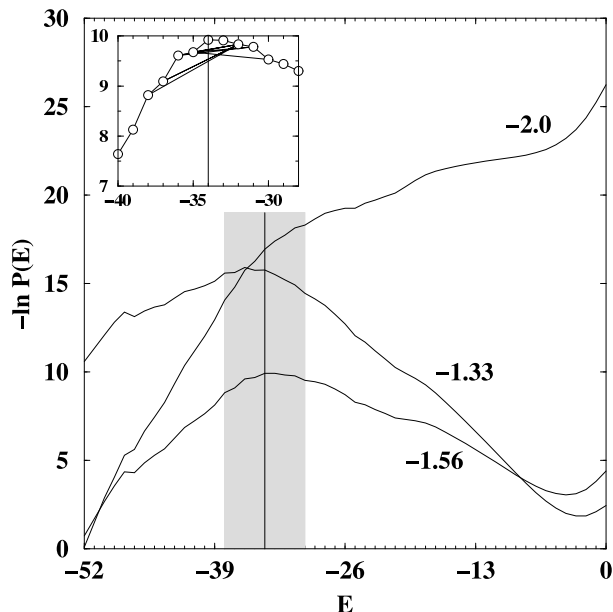


FIG. 2. Free energies profiles are given by negative logarithmic distributions of energy (solid curves), plotted here for the $\epsilon/k_B T$'s shown. $P(E)$ is the sum of Boltzmann weights of conformations with energies E' in the range $E - 0.5 < E' \leq E + 0.5$. The vertical dashed line marks the $E = -34$ free energy peak for $\epsilon/k_B T = -1.56$. The inset shows the peak region of this profile, where lines joining a pair of open circles [$-\ln P(E)$ values] record all single-chain-move interconversions between a conformation with $E < -34$ and one with $E > -33$ in our simulation. These kinetic connections suggest identifying the shaded area ($-38 \leq E \leq -30$) as a transition state region.

As we have discussed from a general polymer perspective,¹⁹ matching theoretical considerations with the experimental practice of calorimetric baseline subtractions necessitate a multiple-conformation native state that entails considerable fluctuations beyond small-amplitude vibrations. Here we further investigate the implications of native-state conformational diver-

sity. To that end, we study different definition of “native” and “denatured” states by assigning different values for a “transition” energy E_t demarcating the native and denatured ensembles, such that $P_N = \sum_{E < E_t} g(E) \exp(\epsilon E/k_B T)/Q$ is the fractional native population and $P_D = 1 - P_N$ is the fractional denatured population (Fig. 1). For each of these definitions to be tested, a range of energies is spanned by the native state, except for the special case when E_t is chosen to be equal to the ground-state energy. Remarkably, despite the differences in the definitions of “native” and “denatured” states, the thermodynamic ($\Delta G = 0$) transition mid-points of the different E_t 's in Fig. 1 are very similar, all at $\epsilon/k_B T \approx -1.56$.

Stabilities of different denatured ensembles relative to that of the ground state are shown in Fig. 1 (dashed curves). These quantities correspond roughly to native state hydrogen exchange (HX) free energies,^{52–54} (see also ref. 55), for it is reasonable to expect that certain amides become exposed and exchangeable when the effective energy of a conformation is above a certain threshold. Our results share the same general trend as that observed in these experiments,^{52–54} suggesting that some of the fluctuations observed by HX may be considered as part of a multiple-conformation native state.^{18,19,56} Figure 1 indicates that linear extrapolation of ΔG from the transition region to the strongly native regime (more negative $\epsilon/k_B T$) is only valid for the free energy difference between the set of “fully unfolded” open conformations and the ground state (top dashed curve).

III. FREE ENERGY PROFILES AND CHEVRON PLOTS

Consistent with the model’s thermodynamically two-state character,²⁰ its energy distribution is bimodal under denaturing conditions and moderately native conditions (Fig. 2), although the distribution becomes one-sided or “downhill”^{7,57,58} under strongly native conditions (e.g., when $\epsilon/k_B T = -2.0$). We emphasize that here the determination of $\ln P(E)$ is entirely independent of any kinetic consideration. Therefore, the present $\ln P(E)$ function reflects the actual thermodynamics of the model. As such, its physical origin is fundamentally different from free energy profiles that have been empirically constructed or postulated to fit rate data. We can therefore use these $\ln P(E)$'s to assess the transition state picture, with E as the reaction coordinate. Different reaction coordinates have been used in other investigations.^{59,60}

We employ standard Metropolis Monte Carlo dynamics^{19,22} to explore physically plausible kinetic scenarios, using the number of attempted moves as the model time. This approach has been proven useful^{7–11,13,61} despite its obvious limitations.^{11,16,50} The present set of elementary chain moves consists of end

flips, corner flips, crankshafts,^{59–61} rigid rotations,¹¹ and local moves that transform two turns of a right-handed helix among its three possible orientations while holding its two end monomers fixed. The relative frequencies of attempting these moves are 2.3%, 27%, 60.6%, 10%, and 0.1%, respectively. Some chain moves can lead to large changes in energy, hence movements along the model free energy profile need not be continuous (inset of Fig. 2). Therefore, it is more justified to regard the transition state as a region rather than a single highest point along this particular reaction coordinate.^{22,26,60} The group of conformations represented by the shaded area in Fig. 2 clearly serves the role of a transition state because all conformational interconversions between the native and unfolded sides of the population distribution must pass through one or more conformations in the shaded area.

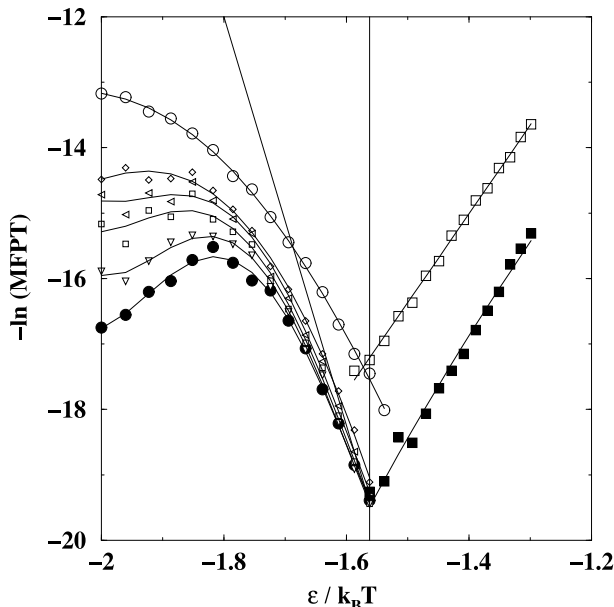


FIG. 3. Model chevron plots. Average logarithmic rates are given by negative logarithms of mean first passage time (MFPT). Each folding trajectory starts from a randomly generated conformation; unfolding trajectories are initiated from the ground state. Each data point is averaged from ~ 50 –1,000 trajectories. Solid curves through data points are mere guides for the eye. Larger squares on the right show unfolding MFPT’s for attaining energies $E > -34$ (open) and $E > -4$ (filled). Unfolding MFPT’s for $E > -10$ are essentially identical to that for $E > -4$. Other data points (on the left) show folding MFPT’s for reaching (from top to bottom) $E \leq -34, -40, -42, -44, -46$, and the ground state. The vertical dashed line is the approximate transition midpoint. The inclined dashed-dotted line shows folding rates if kinetics were two-state for the present model, an hypothetical situation in which the ground state thermodynamic stability relative to the fully unfolded conformations (c.f. dashed line labeled by “-10” in Fig. 1) is given by the difference between logarithmic folding rates (dashed-dotted line) and unfolding rates extrapolated from the solid squares.

Figure 3 reports simulated mean first passage times^{59,60} for a range of intraprotein interaction strength on both sides of the transition midpoint, in a format identical to typical experimental chevron plots.^{29,31,32,49,51,62} We explore a variety of kinetic folding and unfolding criteria by monitoring the time it takes for the chain to first cross several different “finish lines.” This results in an appreciable variation in apparent rates under strongly native conditions (Fig. 3, more negative $\epsilon/k_B T$). Similar effects may be operative when multiple experimental probes are used to monitor kinetics.^{63–65}

The trajectory in Fig. 4 (upper panel) depicts the model’s heuristically “two-state” behavior at the transition midpoint. For the two chain properties shown, native and denatured parts of the trajectory can be easily discerned, with very little time spent in between; strongly suggesting that the kinetics is first order. Fluctuations in E is considerable within the native (low E) part of the trajectory, underscoring the utility and necessity of a multiple-conformation native state (see Fig. 1 and below). Another facet of the native-denatured interconversion is provided by the R_g trace. Consistent with a recent kinetic R_g measurement on a small protein,⁶⁶ it shows that the chain undergoes sharp kinetic transitions between a native state that has minimal fluctuations in R_g and a denatured state that spans a wide range of R_g ’s.

A more quantitative test introduced by Gutin et al.⁶⁷ is performed in the lower panel of Fig. 4. It indicates that folding kinetics is essentially first order (i.e., single-exponential) for an extended range of model intraprotein interaction strength, covering moderately native conditions ($\epsilon/k_B T \approx -1.80$) through conditions that are less favorable to folding (less negative $\epsilon/k_B T$), although deviations from single-exponential behavior occur under strongly native conditions in the model ($\epsilon/k_B T < -1.85$). Using the same technique, unfolding kinetics (Fig. 3) is found to be essentially single-exponential for the entire range of unfolding $\epsilon/k_B T$ investigated (detailed results not shown). We have confirmed these conclusions by analyzing first passage time (FPT) distributions as in ref. 68 at several $\epsilon/k_B T$ ’s, paying special attention to folding kinetics under moderately native conditions that are not far from the onset of drastic chevron rollover and non-single-exponential behavior (Fig. 3). For example, we have obtained the logarithmic FPT distribution at $\epsilon/k_B T = -1.72$ by binning 1,080 simulated trajectories into time slots of 10^6 , and found that 98% of these trajectories can be fitted by a single exponential with a correlation coefficient $r = 0.95$. If one assumes that the unit model time needed for each elementary chain move corresponds roughly to a real time scale of 10^{-11} – 10^{-9} sec (ref. 69), the fastest model folding rate in Fig. 3 is in the order of 10^2 – 10^4 sec⁻¹.

The contrast between the present model and its corresponding Gō model is intriguing. We have shown that the Gō model in Fig. 4 is thermodynamically significantly

less cooperative,²⁰ yet it folds faster than our model. This scenario of a *negative* correlation between folding speed and thermodynamic cooperativity may bear on the issue of folding rate overestimation in folding theories that use $G\bar{o}$ -like potentials.²³ It also raises a more basic question as to whether and when the $G\bar{o}$ prescription is sufficiently adequate for capturing minimal frustration²¹ mechanisms in real proteins.

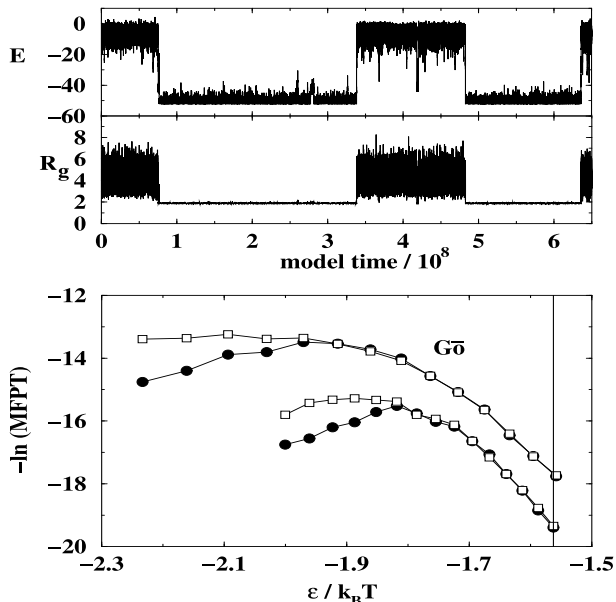


FIG. 4. **Upper panel:** A typical trajectory at $\epsilon/k_B T = -1.56$. R_g is radius of gyration in units of lattice bond length. **Lower panel:** Folding MFPT’s (filled circles) through the ground state for the model in Fig. 3 (lower curves) are compared to that for a $G\bar{o}$ model (upper curves) that has the same transition midpoint (vertical dashed line), uses the same move set, and assigns a -1.5 energy for every contact in the conformation in Fig. 1 and zero energy otherwise. Lines through data points are mere guides for the eye. Open squares are median first passage times divided by $\ln 2$, which equals MFPT for single-exponential kinetics. Hence a discrepancy between the circles and squares signals a deviation from single-exponential kinetics.⁶⁷

The present model is proteinlike in that it predicts a mild chevron rollover concomitant with single-exponential folding kinetics, consistent with experiments.^{29,31,62} But the drastic chevron rollover (with an appreciable decreasing folding rate with increasing native conditions, and non-single-exponential folding kinetics) predicted for strongly native conditions in the present model ($\epsilon/k_B T < -1.85$ in Fig. 3) has not been documented for real proteins. This suggests that such conditions, which coincide with downhill folding^{7,57,58} in the present model (see above), may not be realizable. If so, this is not surprising. Native stability can be arbitrary high in the model ($-\epsilon/k_B T$ can be arbitrarily large), but for real proteins native stability is limited by the actual

chemistry at zero denaturant. It follows that the experimental zero-denaturant situation for most proteins most likely corresponds to $\epsilon/k_B T > -1.80$ in Fig. 3. It would be interesting to explore whether special experimental situations corresponding to the very strongly folding conditions in the model can be found for some proteins such that similar drastic chevron rollovers can be observed.

IV. ASSESSING THE TRANSITION STATE PICTURE

Consistent with the thermodynamics of our model, kinetic rate of folding to the ground state and of unfolding to an open state meet at the approximate transition midpoint determined thermodynamically in Fig. 1 (c.f. the lower “V” in Fig. 3). Interestingly, a similar consistency is seen by matching rates of crossing the peak of the free energy profile in the inset of Fig. 2 in the folding and unfolding directions (upper “V” in Fig. 3). Near the transition midpoint, folding rates defined by crossing several different finish lines at low but non-ground-state energies are very close to one another, and are only slightly faster than the rate of folding to the ground state (Fig. 3). This implies that, under midpoint to moderately native conditions, kinetics is rapid once the folding chain has cleared the shaded transition state region in Fig. 2 and proceeds on to the native side. But the folding rates for different finish lines are very different under strongly native conditions ($\epsilon/k_B T \approx -2.0$), indicative of glassy dynamics (Figs. 3 and 4).

Despite the essentially single-exponential and heuristically “two-state” kinetics discussed above, the folding/unfolding kinetics of the present model differs from the strictly two-state variety observed for an increasing number of small single-domain proteins^{4,5,24,25,70} such as a 64-residue form of chymotrypsin inhibitor 2. Figure 3 shows that folding rates under moderately to strongly native conditions are slower than that required for such strictly thermodynamically *and* kinetically two-state proteins (inclined dashed-dotted line). In fact, Fig. 3 is reminiscent of experimental chevron plots with rollovers.^{31,32,71} Examples include wildtype barnase²⁹ and ribonuclease A.⁶² Hence we believe the present lattice construct may serve as a tool for better understanding the folding kinetics of these proteins.

How much kinetic information can be inferred from free energy profiles such as those in Fig. 2? The conventional transition state picture of protein folding^{2,28,30} stipulates that

$$\text{rate} = F \exp\left(-\frac{\Delta G^\ddagger}{k_B T}\right), \quad (1)$$

where ΔG^\ddagger is the activation free energy for the kinetic process in question. We call $\Delta G^\ddagger/k_B T$ the transition-state exponent. F is the pre-exponential front factor¹¹

or prefactor,²³ which depends on solvent viscosity (not considered here) but is often taken to be insensitive to intraprotein interaction strength.³⁰ Figure 5 examines whether this picture applies to the present model. It does so by investigating the dependence of F on $\epsilon/k_B T$. For the sake of generality, several physically motivated $P(E)$ -based definitions of “transition state,” “folded state” and “unfolded state” are evaluated. In the tests conducted here, “transition state” is defined by either the shaded area in Fig. 2 ($-38 \leq E \leq -30$) or $E = -34$ (peak of barrier); “folded state” is defined by the ground state only ($E = -52$) or by $E \leq -34$ (left of the barrier); and “unfolded state” is defined by the approximate position of the denatured free energy minimum ($E = -4$), by the bulk of the open conformations ($E > -10$), or by $E \geq -34$ (right of the barrier). Transition-state exponents for folding and unfolding are then computed, respectively, by the [transition/unfolded] and [transition/folded] population ratios at the given $\epsilon/k_B T$ (Fig. 5).

The scaling of F with respect to $\epsilon/k_B T$ is found to be not sensitive to these variations in definition (Fig. 5, upper panel). Our results show that the simple transition state picture does not apply to folding in this model. For the quasi-linear part of the chevron plot in Fig. 3, the relationship between $\Delta G^\ddagger/k_B T$ and $-\ln(\text{MFPT})$ is approximately linear (Fig. 5), with slope ≈ -1.5 (filled symbols) or ≈ -1.9 (open symbols). This implies that F has approximately the same functional form as the activation factor in this regime, but with an exponent of opposite sign, viz., $F \sim \exp(-\mu \Delta G^\ddagger/k_B T)$, where $\mu \approx -0.33$ for folding to the ground state (filled symbols). On the other hand, unfolding appears to be well described by the simple transition state picture. The corresponding slope for unfolding ≈ -1.0 , hence $F \approx \text{constant}$. Folding and unfolding front factors are approximately equal near the thermodynamic midpoint (Fig. 5, lower panel), reflecting the fact that in that region folding and unfolding rates are essentially equal (Fig. 3). The role of front factors in understanding folding rates has recently been emphasized by Portman et al.²³ The pattern in Fig. 5 is similar in some respects to the results of a recent model study by Nymeyer et al.²² Using a different reaction coordinate for 2-, 3-letter and G $\bar{5}$ 27mer models, these authors found approximate linear relations with non-unity slopes between kinetically simulated rates and rate quantities deduced from free energy profiles, although they did not consider a broad range of overall interaction strengths as that in chevron plots.

Figure 5 shows that F for folding decreases with increasingly native conditions. F may be identified as an effective diffusion coefficient. It corresponds to an internal friction term arising from the impediment to motion imposed by the chain segments on one another.^{2,7,23,60,71–74} Plaxco and Baker⁷² have experimentally investigated internal friction in protein folding, and concluded insightfully that internal friction effects are limited for strictly

two-state proteins. But the functional form they considered is different from the novel approximate exponential form $F \sim \exp(-\mu \Delta G^\ddagger/k_B T)$ discovered here for the quasi-linear part of chevron plots and the part with a mild rollover (corresponding to a limited range of $\epsilon/k_B T$) for proteins that are not kinetically two-state. In the present model, when a wider range of $\epsilon/k_B T$ is considered (Fig. 5, lower panel), the folding $\ln F$ reveals its nonlinear character, a feature anticipated by energy landscape theory^{21,23} and consistent with a pioneering simulation study of Socci et al.⁶⁰

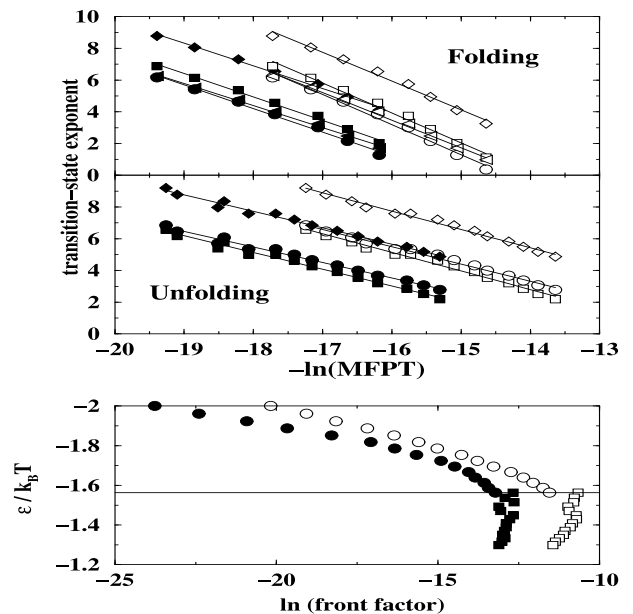


FIG. 5. Correlations between rates and transition-state exponents. Filled symbols are for reaching the ground state in folding and reaching $E > -4$ in unfolding, open symbols are for crossing the $-\ln P(E)$ peak at $E = -34$ in either directions. **Upper panel:** Folding transition-state exponent $\Delta G^\ddagger/k_B T = -\ln[P(-38 \leq E \leq -30)/P(E \geq -10)]$ (circles), $-\ln[P(-38 \leq E \leq -30)/P(E \geq -34)]$ (triangles), $-\ln[P(E = -34)/P(E = -4)]$ (squares), or $-\ln[P(E = -34)/P(E \geq -10)]$ (diamonds). Data points shown are for $\epsilon/k_B T \geq -1.75$. For unfolding, $\Delta G^\ddagger/k_B T = -\ln[P(-38 \leq E \leq -30)/P(E = -52)]$ (squares), $-\ln[P(-38 \leq E \leq -30)/P(E \leq -34)]$ (circles), or $-\ln[P(E = -34)/P(E = -52)]$ (diamonds). The straight lines are fitted. **Lower panel:** $\ln F \equiv -\ln(\text{MFPT}) + \Delta G^\ddagger/k_B T$ (horizontal variable) vs. $\epsilon/k_B T$. Filled and open circles (for folding) and squares (for unfolding) identify the folding and unfolding $\Delta G^\ddagger/k_B T$ used, as defined in the upper panel. The dashed line marks the approximate transition midpoint.

V. THE CALORIMETRIC CONNECTION: WHAT IS THE NATIVE STATE?

A thermodynamic consideration of the model’s free energy profiles (Fig. 2) and the above kinetic analysis

suggest that a natural way to define the “native” and “denatured” states is to have their demarcation line at $E_t = -34$. Figure 6 investigates the calorimetric implications of different E_t choices. As a first test of principles, in this section we take the effective intraprotein energies as temperature independent. Our conclusions are not expected to be significantly altered by the incorporation of proteinlike temperature-dependent effective interactions.¹⁸

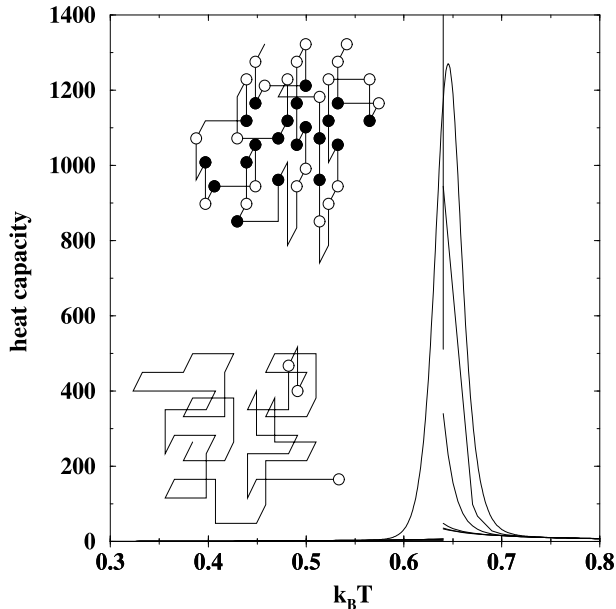


FIG. 6. Heat capacity vs. temperature (from ref. 20). Here nonlinear denatured (high T) dashed baselines^{19,75} are computed for (from top to bottom) $E_t = -52.04, -48, -42, -38$, and -34 (c.f. Fig. 1). Corresponding native baselines are plotted but are too close to one another to be distinguishable. The vertical dotted line marks the approximate transition midpoint used throughout this work. Also shown are example compact non-ground-state conformations with $E = -36.0$ (top) and $E = -46.0$ (bottom). The beads mark monomers that are not in their folded environment, i.e., do not have their full set of contacts as that in the ground state.

We have argued that empirical calorimetric baseline subtractions correspond essentially to an operational definition of the native and denatured ensembles.¹⁹ The demarcation energy (or enthalpy) between the native and denatured states may be ascertained by matching empirical baselines¹⁹ to the nonlinear “formal two-state” baselines of Zhou et al.⁷⁵ Figure 6 shows that the baselines from empirically extrapolating the native and denatured tails of the heat capacity curve of the present model²⁰ essentially coincide with the formal two-state baselines for $E_t = -34$, implying that by adopting such empirical baselines $E_t = -34$ is effectively adopted. In that case, the two chain conformations shown in Fig. 6 would belong to the native state and therefore may be regarded as sitting “below the calorimetric baseline.”¹⁹

These chains may model the sparsely populated conformations revealed by native-state HX.^{52–54} A multiple-conformation native state view is supported by a recent experimental observation of pretransitional conformational changes in ribonuclease A.⁷⁶

VI. DISCUSSION

The logic of the present analysis is premised on a comparison between simulated folding/unfolding rates and transition-state predictions based on independently obtained free energy profiles. The conventional transition state picture of folding posits a weak or nonexistent dependence of the front factor on a protein’s intrachain interaction strength. In the present model, which exhibits a chevron rollover, we find that the conventional picture holds approximately for unfolding but not for folding. In particular, for the quasi-linear part of the folding arm of the chevron plot, the folding front factor adopts a rescaled form of the exponential factor, harboring an exponent opposite in sign to that of the activation term. These findings are consistent with internal friction and diffusive folding dynamics ideas from energy landscape theory. They suggest that simple transition state theory with a constant front factor may not be generally applicable in the presence of a chevron rollover, even if the kinetics is apparently first order. In this regard, future single-molecule measurements⁷⁷ of folding time distributions may provide important insight into the physics underlying approximate single-exponential folding kinetics, since these measurements may detect small deviations from first-order kinetics¹¹ (e.g., a possible small non-exponential tail in the distribution) that would otherwise be difficult to ascertain from traditional measurements of ensemble-averaged folding rates.

Chevron rollovers have been rationalized by dead-time discrete intermediates²⁹ and by movements of the transition-state peak on broad activation barriers.³¹ We have not been able to detect these proposed features in our model free energy profiles. Instead, the present results offer an alternate rationalization in terms of diffusive dynamics and an interaction-dependent folding front factor. It follows that, in general, analyses that focus exclusively on free energy profiles may be incomplete. Inasmuch as chevron rollovers are a manifestation of an interaction-dependent front factor, as suggested here, experimental observations of significant mutational effects on rollover behavior²⁹ imply that mutations can have a significant effect not only on the free energy profile itself, but also on front factors not afforded by such profiles.

The present account of salient features of chevron rollover and native-state HX in terms of an essentially continuous energy distribution (Fig. 3) is similar in spirit to the recent idea that these features may originate from a “burst phase continuum.”^{32,33} However, the burst

phase continuum view is based on postulated free energy profiles, not free energy profiles derived from models with explicit chain representations. Further effort will be required to elucidate the relationship between the burst phase continuum and the present chain-based perspectives, as there are apparent differences between the two. For instance, the present study suggests that some of the states detected by native-state HX are on the native side of the conformational distribution (Figs. 3 and 6) rather than on the denatured side as envisioned by the burst phase continuum scenario.

In summary, we emphasize that while the current study proposes a new physical rationalization for chevron rollover, it does not by itself rule out other mechanisms. Chevron rollovers in real proteins may arise from a combination of effects. Obviously, the generality of the present interaction-dependent front factor scenario should be further tested using model proteins with non-helical native topologies as well as using geometrically more realistic off-lattice continuum models.^{26,78}

As for the relationship between generic features of folding/unfolding kinetics and thermodynamics of small globular proteins, the qualitative agreement between Fig. 3 and typical chevron rollover plots for real proteins supports the idea that proteinlike thermodynamics necessarily lead to proteinlike folding/unfolding kinetics. A case in point is the folding kinetics of a set of 20-letter model sequences reported by Gutin et al.⁶⁷ Our test calculations show that random sequences of this particular 20-letter alphabet with additive contact energies are not calorimetrically two-state (data not shown). Although much useful insight has been gained from them^{10,14,68} (see also ref. 16), recent calculations¹⁹ indicate that even some designed sequences in this 20-letter model are thermodynamically less cooperative than the present model.²⁰ Apparently, the folding kinetics of these 20-letter model sequences are less proteinlike as a result, in that their folding rates *decrease* when native stability is increased from the transition midpoint (Figs. 2, 5, 7 and 8 in ref. 67). This is because the maximum folding rates and the onset of drastic rollover in these 20-letter models occur around the thermodynamic transition midpoint, rather than under strongly native conditions as in the cooperative model studied here (Fig. 3 of the present work). Thus, the chevron trend predicted by these 20-letter models under transition midpoint through moderately folding conditions is opposite to that observed experimentally,^{49,51} because experiments almost invariably show an increasing folding rate when native stability is increased from the transition midpoint.

The present model's kinetics is proteinlike but not two-state. In this respect, it is reassuring that the exercise here fares no worse than Nature's. This is because a protein's calorimetric two-state cooperativity,⁷⁹ such as that of hen lysozyme,^{63,71} barnase,²⁹ and ribonuclease A,⁶² is no guarantee for two-state kinetics.^{4,5} However,

the present exercise does suggest that additional or alternate interaction mechanisms have to be discovered to account for the strictly two-state behavior of many small single-domain proteins. In that regard, it would be interesting to investigate the connection between the strictly two-state proteins' apparently nonglassy kinetics⁸⁰ and the possibility that their front factors might be minimally sensitive to the variation in intrachain interaction strength.

Acknowledgments

We thank Alan Davidson, Julie Forman-Kay, Yuji Goto, Bob Matthews, and Tetsuya Yomo for helpful discussions, and David Baker, Martin Gruebele, Walid Houry, Kevin Plaxco, and Peter Wolynes for their critical reading of an earlier draft of this paper and their very useful suggestions. This work was supported by Medical Research Council of Canada grant no. MT-15323 and a Premier's Research Excellence Award (Ontario). H. S. C. is a Canada Research Chair in Biochemistry.

-
- [1] Baker, D. (2000). A surprising simplicity to protein folding. *Nature* **405**, 39–42.
 - [2] Bilsel, O. & Matthews, C. R. (2000). Barriers in protein folding reactions. *Adv. Protein Chem.* **53**, 153–207.
 - [3] Eaton, W. A., Muñoz, V., Hagen, S. J., Jas, G. S., Lapidus, L. J., Henry, E. R. & Hofrichter, J. (2000). Fast kinetics and mechanisms in protein folding. *Annu. Rev. Biophys. Biomolec. Struct.* **29**, 321–359.
 - [4] Fersht, A. R. (2000). Transition-state structure as a unifying basis in protein-folding mechanisms: Contact order, chain topology, stability, and the extended nucleus mechanism. *Proc. Natl. Acad. Sci. USA* **97**, 1525–1529.
 - [5] Plaxco, K. W., Simons, K. T., Ruczinski, I. & Baker, D. (2000). Topology, stability, sequence, and length: Defining the determinants of two-state protein folding kinetics. *Biochemistry* **39**, 11177–11183.
 - [6] Radford, S. E. (2000). Protein folding: progress made and promises ahead. *Trend Biochem. Sci.* **25**, 611–618.
 - [7] Bryngelson, J. D., Onuchic, J. N., Socci, N. D. & Wolynes, P. G. (1995). Funnels, pathways, and the energy landscape of protein folding: A synthesis. *Proteins Struct. Funct. Genet.* **21**, 167–195.
 - [8] Dill, K. A., Bromberg, S., Yue, K., Fiebig, K. M., Yee, D. P., Thomas, P. D. & Chan, H. S. (1995). Principles of protein folding — A perspective from simple exact models. *Protein Sci.* **4**, 561–602.
 - [9] Thirumalai, D. & Woodson S. A. (1996). Kinetics of folding of proteins and RNA. *Acc. Chem. Res.* **29**, 433–439.
 - [10] Shakhnovich, E. I. (1997). Theoretical studies of protein folding thermodynamics and kinetics. *Curr. Opin. Struct. Biol.* **7**, 29–40.
 - [11] Chan, H. S. & Dill, K. A. (1998). Protein folding in the landscape perspective: Chevron plots and non-Arrhenius kinetics. *Proteins Struct. Funct. Genet.* **30**, 2–33.

- [12] Micheletti, C., Banavar, J. R., Maritan, A. & Seno, F. (1999). Protein structures and optimal folding from a geometrical variational principle. *Phys. Rev. Lett.* **82**, 3372–3375.
- [13] Onuchic, J. N., Nymeyer, H., Garcia, A. E., Chahine, J. & Socci, N. D. (2000). The energy landscape theory of protein folding: Insights into folding mechanisms and scenarios. *Adv. Protein Chem.* **53**, 87–152.
- [14] Mirny, L. & Shakhnovich, E. (2001). Protein folding theory: From lattice to all-atom models. *Annu. Rev. Biophys. Biomol. Struct.* **30**, 361–396.
- [15] Thirumalai, D. & Lorimer, G. H. (2001). Chaperonin-mediated protein folding. *Annu. Rev. Biophys. Biomol. Struct.* **30**, 245–269.
- [16] Chan, H. S., Kaya, H. & Shimizu, S. (2002). Computational methods for protein folding: Scaling a hierarchy of complexities. In *Current Topics in Computational Molecular Biology*, eds. Jiang, T., Xu, Y. & Zhang, M. Q. (The MIT Press, Cambridge, MA), pp. 403–447.
- [17] Chan, H. S. (1998). Matching speed and locality. *Nature* **392**, 761–763.
- [18] Chan, H. S. (2000). Modeling protein density of states: Additive hydrophobic effects are insufficient for calorimetric two-state cooperativity. *Proteins Struct. Funct. Genet.* **40**, 543–571.
- [19] Kaya, H. & Chan, H. S. (2000). Polymer principles of protein calorimetric two-state cooperativity. *Proteins Struct. Funct. Genet.* **40**, 637–661 [Erratum: **43**, 523 (2001)].
- [20] Kaya, H. & Chan, H. S. (2000). Energetic components of cooperative protein folding. *Phys. Rev. Lett.* **85**, 4823–4826.
- [21] Bryngelson, J. D. & Wolynes, P. G. (1987). Spin glasses and the statistical mechanics of protein folding. *Proc. Natl. Acad. Sci. USA* **84**, 7524–7528.
- [22] Nymeyer, H., Socci, N. D. & Onuchic, J. N. (2000). Landscape approaches for determining the ensemble of folding transition states: Success and failure hinge on the degree of frustration. *Proc. Natl. Acad. Sci. USA* **97**, 634–639.
- [23] Portman, J. J., Takada, S. & Wolynes, P. G. (2001). Microscopic theory of protein folding rates. II. Local reaction coordinates and chain dynamics. *J. Chem. Phys.* **114**, 5082–5096.
- [24] Alm, E. & Baker, D. (1999). Prediction of protein-folding mechanisms from free-energy landscapes derived from native structures. *Proc. Natl. Acad. Sci. USA* **96**, 11305–11310.
- [25] Muñoz, V. & Eaton, W. A. (1999). A simple model for calculating the kinetics of protein folding from three-dimensional structures. *Proc. Natl. Acad. Sci. USA* **96**, 11311–11316.
- [26] Clementi, C., Nymeyer, H. & Onuchic, J. N. (2000). Topological and energetic factors: What determines the structural details of the transition state ensemble and “en-route” intermediates for protein folding? An investigation for small globular proteins. *J. Mol. Biol.* **298**, 937–953.
- [27] Myers, J. K. & Oas, T. G. (2001). Preorganized secondary structure as an important determinant of fast protein folding. *Nature Struct. Biol.* **8**, 552–558.
- [28] Matthews, C. R. & Hurle, M. R. (1987). Mutant sequences as probes of protein folding mechanisms. *BioEssays* **6**, 254–257.
- [29] Matouschek, A., Kellis, J. T., Serrano, L., Bycroft, M. & Fersht, A. R. (1990). Characterizing transient folding intermediates by protein engineering. *Nature* **346**, 440–445.
- [30] Fersht, A. R., Matouschek, A. & Serrano, L. (1992). The folding of an enzyme. I. Theory of protein engineering analysis of stability and pathway of protein folding. *J. Mol. Biol.* **224**, 771–782.
- [31] Oliveberg, M. (1998). Alternative explanations for “multistate” kinetics in protein folding: Transient aggregation and changing transition-state ensembles. *Acc. Chem. Res.* **31**, 765–772.
- [32] Parker, M. J. & Marqusee, S. (1999). The cooperativity of burst phase reactions explored. *J. Mol. Biol.* **293**, 1195–1210.
- [33] Parker, M. J. & Marqusee, S. (2000). A statistical appraisal of native state hydrogen exchange data: Evidence for a burst phase continuum? *J. Mol. Biol.* **300**, 1361–1375.
- [34] Wang, J. & Wang, W. (1999). A computational approach to simplifying the protein folding alphabet. *Nature Struct. Biol.* **6**, 1033–1038.
- [35] Klimov, D. K., Betancourt, M. R. & Thirumalai, D. (1998). Virtual atom representation of hydrogen bonds in minimal off-lattice models of α helices: effect on stability, cooperativity and kinetics. *Fold. Des.* **3**, 481–496.
- [36] Takada, S., Luthey-Schulten, Z. & Wolynes, P. G. (1999). Folding dynamics with nonadditive forces: A simulation study of a designed helical protein and a random heteropolymer. *J. Chem. Phys.* **110**, 11616–11629.
- [37] Kolinski, A., Galazka, W. & Skolnick, J. (1996). On the origin of the cooperativity of protein folding: Implications from model simulations. *Proteins Struct. Funct. Genet.* **26**, 271–287.
- [38] Hao, M.-H. & Scheraga, H. A. (1997). Characterization of foldable protein models: Thermodynamics, folding kinetics and force field. *J. Chem. Phys.* **107**, 8089–8102.
- [39] Eastwood, M. P. & Wolynes, P. G. (2001). Role of explicitly cooperative interactions in protein folding funnels: A simulation study. *J. Chem. Phys.* **114**, 4702–4716.
- [40] Rank, J. A. & Baker, D. (1997). A desolvation barrier to hydrophobic cluster formation may contribute to the rate-limiting step in protein folding. *Protein Sci.* **6**, 347–354.
- [41] Czaplowski, C., Rodziewicz-Motowidlo, S., Liwo, A., Ripoll, D. R., Wawak, R. J. & Scheraga, H. A. (2000). Molecular simulation study of cooperativity in hydrophobic association. *Protein Sci.* **9**, 1235–1245.
- [42] Shimizu, S. & Chan, H. S. (2000). Temperature dependence of hydrophobic interactions: A mean force perspective, effects of water density, and non-additivity of thermodynamic signatures. *J. Chem. Phys.* **113**, 4683–4700.
- [43] Shimizu, S. & Chan, H. S. (2001). Configuration-dependent heat capacity of pairwise hydrophobic interactions. *J. Am. Chem. Soc.* **123**, 2083–2084.
- [44] Shimizu, S. & Chan, H. S. (2001). Anti-cooperativity in hydrophobic interactions: A simulation study of spatial dependence of three-body effects and beyond. *J. Chem. Phys.* **115**, 1414–1421.

- [45] Shimizu, S. & Chan, H. S. (2001). Statistical mechanics of solvophobic aggregation: Additive and cooperative effects. *J. Chem. Phys.* **115**, 3424–3431.
- [46] Bromberg, S. & Dill, K. A. (1994). Sidechain entropy and packing in proteins. *Protein Sci.* **3**, 997–1009.
- [47] Klimov, D. K. & Thirumalai, D. (1998). Cooperativity in protein folding: From lattice models with sidechains to real proteins. *Fold. & Des.* **3**, 127–139.
- [48] Alonso, D. O. V. & Dill, K. A. (1991). Solvent denaturation and stabilization of globular proteins. *Biochemistry* **30**, 5974–5985.
- [49] Scalley, M. L. & Baker, D. (1997). Protein folding kinetics exhibit an Arrhenius temperature dependence when corrected for the temperature dependence of protein stability. *Proc. Natl. Acad. Sci. USA* **94**, 10636–10640.
- [50] Chan, H.S. (1998). Modelling protein folding by Monte Carlo dynamics: Chevron plots, chevron rollover, and non-Arrhenius kinetics. In *Monte Carlo Approach to Biopolymers and Protein Folding* (Grassberger, P., Barkema, G.T. & Nadler, W., eds) pp. 29–44, World Scientific, Singapore.
- [51] Kuhlman, B., Luisi, D. L., Evans, P. A. & Raleigh, D. P. (1998). Global analysis of the effects of temperature and denaturant on the folding and unfolding kinetics of the N-terminal domain of the protein L9. *J. Mol. Biol.* **284**, 1661–1670.
- [52] Kim, K. S. & Woodward, C. (1993). Protein internal flexibility and global stability: Effect of urea on hydrogen-exchange rates of bovine pancreatic trypsin inhibitor. *Biochemistry* **32**, 9609–9613.
- [53] Bai, Y., Sosnick, T. R., Mayne, L. & Englander, S. W. (1995). Protein folding intermediates: Native-state hydrogen exchange. *Science* **269**, 192–197.
- [54] Llinás, M., Gillespie, B., Dahlquist, F. W. & Marqusee, S. (1999). The energetics of T4 lysozyme reveal a hierarchy of conformations. *Nature Struct. Biol.* **6**, 1072–1078.
- [55] Miller, D. W. & Dill, K. A. (1995). A statistical mechanical model for hydrogen exchange in globular proteins. *Protein Sci.* **4**, 1860–1873.
- [56] Sadqi, M., Casares, S., Abril, M. A., López-Mayorga, O., Conejero-Lara, F. & Freire, E. (1999). The native state conformational ensemble of the SH3 domain from α -spectrin. *Biochemistry* **38**, 8899–8906.
- [57] Eaton, W. A. (1999). Searching for “downhill scenarios” in protein folding. *Proc. Natl. Acad. Sci. USA* **96**, 5897–5899.
- [58] Sabelko, J., Ervin, J. & Gruebele, M. (1999). Observation of strange kinetics in protein folding. *Proc. Natl. Acad. Sci. USA* **96**, 6031–6036.
- [59] Šali, A., Shakhnovich, E. & Karplus, M. (1994). How does a protein fold. *Nature* **369**, 248–251.
- [60] Socci, N. D., Onuchic, J. N. & Wolynes, P. G. (1996). Diffusive dynamics of the reaction coordinate for protein folding funnels. *J. Chem. Phys.* **104**, 5860–5868.
- [61] Pande, V. S. & Rokhsar, D. S. (1999). Folding pathway of a lattice model for proteins. *Proc. Natl. Acad. Sci. USA* **96**, 1273–1278.
- [62] Houry, W. A., Rothwarf, D. M. & Scheraga, H. A. (1995). The nature of the initial step in the conformational folding of disulphide-intact ribonuclease A. *Nature Struct. Biol.* **2**, 495–503.
- [63] Dobson, C. M., Evans, P. A. & Radford, S. E. (1994). Understanding how proteins fold: The lysozyme story so far. *Trend Biochem. Sci.* **19**, 31–37.
- [64] Arai, M. & Kuwajima, K. (2000). Role of the molten globule state in protein folding. *Adv. Protein Chem.* **53**, 209–282.
- [65] Kuwata, K., Shastry, R., Cheng, H., Hoshino, M., Batt, C. A., Goto, Y. & Roder, H. (2001). Structural and kinetic characterization of early folding events in β -lactoglobulin. *Nature Struct. Biol.* **8**, 151–155.
- [66] Plaxco, K. W., Millett, I. S., Segel, D. J., Doniach, S. & Baker, D. (1999). Chain collapse can occur concomitantly with the rate-limiting step in protein folding. *Nature Struct. Biol.* **6**, 554–556.
- [67] Gutin, A., Sali, A., Abkevich, V., Karplus, M. & Shakhnovich, E. I. (1998). Temperature dependence of the folding rate in a simple protein model: Search for a “glass” transition. *J. Chem. Phys.* **108**, 6466–6483.
- [68] Abkevich, V. I., Gutin, A. M. & Shakhnovich, E. I. (1994). Free energy landscape for protein folding kinetics: Intermediates, traps, and multiple pathways in theory and lattice model simulations. *J. Chem. Phys.* **101**, 6052–6062.
- [69] Creighton, T. E. (1984). *Proteins — Structures and Molecular Properties* pp. 180–181, W. H. Freeman and Co., New York.
- [70] Debe, D. A. & Goddard, W. A. (1999). First principles prediction of protein folding rates. *J. Mol. Biol.* **294**, 619–625.
- [71] Kiefhaber, T. (1995). Kinetic traps in lysozyme folding. *Proc. Natl. Acad. Sci. USA* **92**, 9029–9033.
- [72] Plaxco, K. W. & Baker, D. (1998). Limited internal friction in the rate-limiting step of a two-state protein folding reaction. *Proc. Natl. Acad. Sci. USA* **95**, 13591–13596.
- [73] Tüzel, E. & Erzan, A. (2000). Glassy dynamics of protein folding. *Phys. Rev. E* **61**, R1040–R1043.
- [74] Jacob, M., Geeves, M., Holtermann, G. & Schmid, F. X. (1999). Diffusional barrier crossing in a two-state protein folding reaction. *Nature Struct. Biol.* **6**, 923–926.
- [75] Zhou, Y., Hall, C. K. & Karplus, M. (1999). The calorimetric criterion for a two-state process revisited. *Protein Sci.* **8**, 1064–1074.
- [76] Stelea, S. D., Pancoska, P., Benight, A. S. & Keiderling, T. A. (2001). Thermal unfolding of ribonuclease A in phosphate at neutral pH: Deviations from the two-state model. *Protein Sci.* **10**, 970–978.
- [77] Lu, H. P., Xun, L. Y. & Xie, X. S. (1998). Single-molecule enzymatic dynamics. *Science* **282** 1877–1882.
- [78] Thirumalai, D. & Klimov, D. K. (1999). Deciphering the timescales and mechanisms of protein folding using minimal off-lattice models. *Curr. Opin. Struct. Biol.* **9**, 197–207.
- [79] Makhatadze, G. I. & Privalov, P. L. (1995). Energetics of protein structure. *Adv. Protein Chem.* **47**, 307–425.
- [80] Gillespie, B. & Plaxco, K. W. (2000). Nonglassy kinetics in the folding of a simple single-domain protein. *Proc. Natl. Acad. Sci. USA* **97**, 12014–12019.